Binding energies of ground and excited donor states bound to *X* valleys in GaAs/AlAs type-II quantum wells

Gleise N. Carneiro
Faculdade de Engenharia de Joinville, Universidade do Estado de Santa Catarina, Caixa Postal 631, 89223-100 Joinville, SC, Brazil

Gerald Weber
Faculdade de Engenharia, Universidade São Francisco, 13251-900 Itatiba, SP, Brazil
(Received 13 April 1998)

We calculate the binding energies of $1s$, $2s$, $2p_x$, $2p_y$, and $2p_z$ donor states bound to *X* valleys in type-II GaAs-AlAs quantum well structures using an anisotropic variational method that enables us to take into account the effective-mass anisotropy and the quantum confinement. These binding energies present a strong dependence on the effective mass and the valley symmetry. Intradonor $1s \rightarrow 2p$ transitions energies are shown to be up to 1000 cm^{-1}, which is well above the energies usually observed for donors in type-I quantum structures. [S0163-1829(98)04635-9]

I. INTRODUCTION

Type-II quantum well structures, where the lowest energy transition is indirect in real space, have attracted considerable attention in recent years due to their distinguished electrical and optical properties. For instance, such structures can be obtained with $Al_xGa_{1-x}As$/AlAs quantum wells where the Γ states in the $Al_xGa_{1-x}As$ layers are higher in energy than the *X* states in the AlAs layers by an appropriate choice of Al concentrations and layer thickness. Therefore, the electrical and optical properties of type-II structures are very different from their type-I counterparts. In particular, substitutional shallow donors will not be linked to the Γ valley, but to the lower lying *X* valleys.[1] Furthermore, these valleys are no longer degenerate, but the X_z and $X_{x,y}$ valleys will split into different energies due to the quantum confinement in the growth (z) direction and due to biaxial strain effects.

Theoretical studies on shallow impurities in quantum wells used mainly variational techniques,[2,3] which have compared successfully with measurements in several experimental situations,[4–8] and were concentrated mainly on GaAs-$Al_xGa_{1-x}As$ type-I quantum wells. Since the successful growth of *n*-type Si-doped GaAs-AlAs structures[9] the calculation of these binding energies has become important for the understanding of bistable shallow-deep silicon donors in GaAs-AlAs,[10] silicon interdiffusion,[11] and photoluminescence spectra such as those obtained by Lee *et al.*[12] So far, few attempts have been made to understand theoretically impurities in type-II quantum well; for instance, da Cunha Lima *et al.*[13] considered the effect of type-I to type-II transitions for shallow donors at the Γ valley in GaAs quantum wells and in a previous paper we obtained the ground states for donors in type-II structures.[14]

In this paper we calculate the binding energy of hydrogeniclike excited donor states bound to the $X_{x,y}$ and X_z valleys in type-II GaAs-AlAs quantum wells using an anisotropic variational method. Our calculation is expected to be appropriate for substitutional group-IV donors such as Si in AlAs where the effect of valley mixing or central-cell correction can be neglected.[1] We consider the effective-mass anisotropy and the quantum confinement in the growth direction and vary the impurity position along the AlAs layer. Lattice-mismatch-induced strain should have little effect on the donor binding energies and, for simplicity, is not included in this calculation.

A recent high-magnetic cyclotron resonance (CR) experiment by Goiran *et al.*[15] measured *X*-valley effective masses for AlAs that are much heavier than the commonly used values obtained from Faraday rotation (FR) studies;[16,17] see Table I. It is still being debated if there is a camel's back energy structure along the *X* direction,[18] in which case each set of effective masses would belong to closely spaced minima in the *X* direction.[15] We present our results for both sets of effective masses for a comparative study.

In order to form a type-II GaAs-AlAs quantum well we need GaAs layers narrow enough in order to have the confined Γ state (in the GaAs layer) higher in energy than the confined *X* state (in the AlAs layer). Any electron in this Γ state will thus be transferred within picoseconds into the lower lying *X* state.[19] While the quantum wells formed by the Γ valleys may interact strongly for sufficiently narrow AlAs layers, the quantum wells in the *X* valleys are essentially isolated due to the heavy *X* masses involved. There-

TABLE I. Transversal and longitudinal values of effective masses (in units of m_0), effective Bohr radii (in Å), and effective Rydberg energies (in meV) and relations between longitudinal and transversal values and the *x*, *y*, and *z* components for different *X* valleys.

	$m_\perp^*$	$m_\parallel^*$	$a_\perp^*$	$a_\parallel^*$	$R_\perp^*$	$R_\parallel^*$
CR experiment	0.44	2.61	12.03	2.02	59.86	356.47
FR experiment	0.19	1.1	27.85	4.81	25.85	149.7
X_z valley	$m_{x,y}^*$	m_z^*	$a_{x,y}^*$	a_z^*	$R_{x,y}^*$	R_z^*
X_x valley	$m_{x,z}^*$	m_y^*	$a_{x,z}^*$	a_y^*	$R_{x,z}^*$	R_y^*
X_y valley	$m_{y,z}^*$	m_x^*	$a_{y,z}^*$	a_x^*	$R_{y,z}^*$	R_x^*

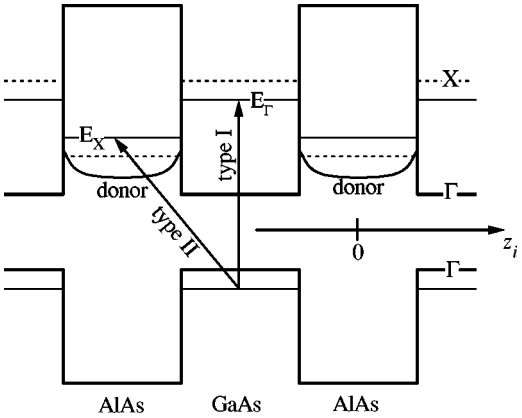

FIG. 1. Schematic diagram for the X-valley donor impurity binding energy and the X (dashed lines) and Γ (solid lines) bulk band alignments. Also shown are the interband transitions from the heavy hole subband to the first Γ confined state (E_Γ) defined as a type-I transition and to the first X confined state (E_X) defined as a type-II transition. The impurity position z_i is centered at the AlAs layer.

fore, in order to calculate electron energy states in GaAs-AlAs type-II quantum wells it is reasonable to consider these X quantum wells as isolated even for narrow GaAs layers.

This paper is organized as follows. In Sec. II we describe the main aspects of the theory used in our calculations. In Sec. III we present our numerical results and discussions. In Sec. IV we draw our conclusions.

II. THEORY

For each of the three valleys X_x, X_y, and X_z we need to write an independent Hamiltonian, which can be written in a single form

$$H_v=-\frac{\hbar^2}{2}\left(\frac{1}{m_x^*}\frac{\partial^2}{\partial x^2}+\frac{1}{m_y^*}\frac{\partial^2}{\partial y^2}+\frac{1}{m_z^*}\frac{\partial^2}{\partial z^2}\right)-\frac{e^2}{4\pi\epsilon[x^2+y^2+(z-z_i)^2]^{1/2}}+V(z), \tag{1}$$

where $v=x,y,z$ (i.e., $X_v=X_x,X_y,X_z$) and $m_{x,y,z}$ are the effective masses along the x,y,z directions. Unlike type-I GaAs-$Al_xGa_{1-x}As$ quantum wells, in our case z is centered in the AlAs layer, i.e., at the center of the X quantum well (see Fig. 1).

We use a standard variational method for the calculation of X impurity states such as in Ref. 2 and we use an anisotropic hydrogenic part of the trial wave functions

$$\Gamma_{v,1s}(x,y,z)=e^{-\alpha_{v,1s}}, \tag{2a}$$

$$\Gamma_{v,2s}(x,y,z)=(1-\beta_{v,2s}\alpha_{v,2s})e^{-\alpha_{v,2s}}, \tag{2b}$$

$$\Gamma_{v,2p_x}(x,y,z)=xe^{-\alpha_{v,2p_x}}, \tag{2c}$$

$$\Gamma_{v,2p_y}(x,y,z)=ye^{-\alpha_{v,2p_y}}, \tag{2d}$$

$$\Gamma_{v,2p_z}(x,y,z)=ze^{-\alpha_{v,2p_z}}, \tag{2e}$$

with

$$\alpha_{v\sigma}=[x^2/a_{v\sigma}^2+y^2/b_{v\sigma}^2+(z-z_i)^2/c_{v\sigma}^2]^{1/2}, \tag{3}$$

where the impurity position z_i is centered in the AlAs layer along the growth direction and $\sigma=1s,2s,2p_x,2p_y,2p_z$. We have labeled these trial function in accordance with their bulk hydrogenic limits, although they should not be identified with actual hydrogenic states since the donor wave function is modified by the barrier potential.[2] The trial function is the one-electron wave function of the quantum well without impurity times the hydrogeniclike part

$$\psi_{v\sigma}(x,y,z)=N_{v\sigma}(z)\phi_v(z)\Gamma_{v\sigma}(x,y,z), \tag{4}$$

$$\phi_v(z)=\begin{cases}\exp[k_{Bv}(z+L/2)], & z\leqslant -L/2\\ \alpha_v\cos(k_{Wv}z), & -L/2<z<L/2\\ \exp[-k_{Bv}(z-L/2)], & z\geqslant -L/2,\end{cases} \tag{5}$$

and

$$k_{Bv}=[2m_z(V_B-E_v)]^{1/2}/\hbar, \tag{6}$$

$$k_{Wv}=(2m_zE_v)^{1/2}/\hbar, \tag{7}$$

with E_v being the quantum well ground state for the valley X_v.

We consider three variational parameters $a_{v\sigma}$, $b_{v\sigma}$, and $c_{v\sigma}$ that enable us to take fully into account the anisotropy of the effective masses as well as the quantum confinement in the z direction. The adimensional parameter β is obtained by requiring that the $1s$ and $2s$ hydrogenic parts of the trial functions are orthogonal.[2]

The binding energy is obtained by minimizing the expected energy

$$E_{v\sigma}(a_{v\sigma},b_{v\sigma},c_{v\sigma})=\frac{\langle\psi_{v\sigma}|H_v|\psi_{v\sigma}\rangle}{\langle\psi_{v\sigma}|\psi_{v\sigma}\rangle} \tag{8}$$

with respect to the three variational parameters $a_{v\sigma}$, $b_{v\sigma}$, and $c_{v\sigma}$. The binding energy is written as

$$E_{\rm BE}=E_v-E_{v\sigma}(a_{v\sigma},b_{v\sigma},c_{v\sigma}). \tag{9}$$

The calculation of $\langle\psi_{v\sigma}|H_v|\psi_{v\sigma}\rangle$ is a straightforward but tedious procedure and will not be shown here. Unlike type-I quantum wells, some terms cannot be calculated analytically; most notably the impurity potential related term

$$I=\langle\psi_{v\sigma}|-\frac{e^2}{4\pi\epsilon[x^2+y^2+(z-z_i)^2]^{1/2}}|\psi_{v\sigma}\rangle \tag{10}$$

has to be calculated by a numerical integration. This triple integration, the minimization of three variational parameters and other numerical integrals not shown here, accounts for a heavy computational effort in order to calculate these donor binding energies accurately.

III. RESULTS AND DISCUSSION

In our calculations we use, for AlAs, a dielectric constant ϵ of 10.0 and a barrier height of 316 meV and consider a band alignment of 35–65 %. The bottom of the bulk X AlAs band edge is thus 145 meV above the bulk Γ GaAs band

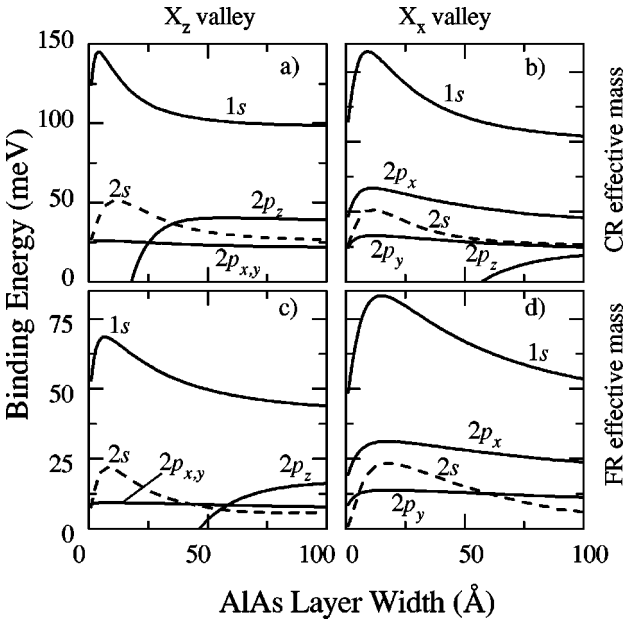

FIG. 2. Binding energies of donors located at the center ($z_i = 0$) of the AlAs layer as a function of the layer width: (a) X_z and (b) X_x valleys calculated with CR effective mass and (c) X_z and (d) X_x valleys calculated with FR effective mass. The $2s$ binding energy is set as a dashed curve for clarity.

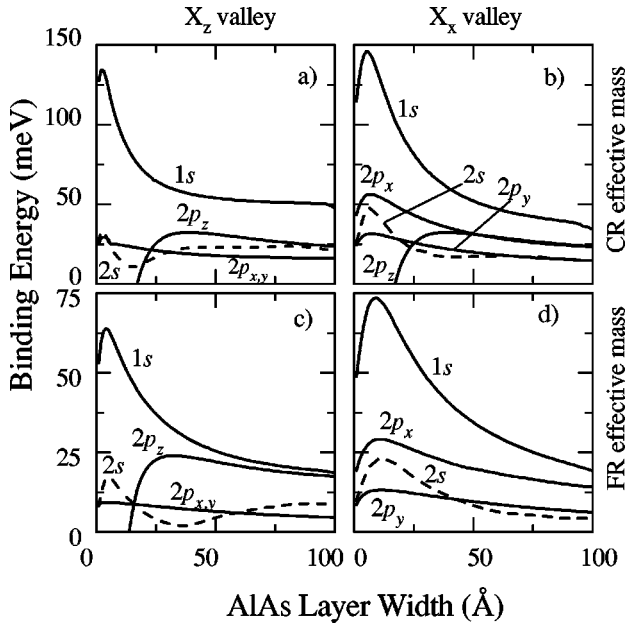

FIG. 3. Binding energies of donors located at the edge ($z_i = L/2$) of the AlAs layer as a function of the layer width: (a) X_z and (b) X_x valleys calculated with CR effective mass and (c) X_z and (d) X_x valleys calculated with FR effective mass. The $2s$ binding energy is set as a dashed curve for clarity.

edge.[17,19] The actual values of the effective masses $m^*_{x,y,z}$ in Eq. (1) depend on the X valley that is being considered. The two sets of bulk AlAs effective masses ($m^*_\perp$, $m^*_\parallel$) and the correspondent $m^*_{x,y,z}$ masses used for each valley are summarized in Table I. For instance, for a X_x valley the effective masses to be used in Eq. (1) are $m^*_x = m^*_\perp$, $m^*_y = m^*_\parallel$, and $m^*_z = m^*_\perp$; if bulk AlAs masses $m^*_{\perp,\parallel}$ are taken from the FR experimental values then we will be using $m^*_x = 0.19m_0$, $m^*_y = 1.1m_0$, and $m^*_z = 0.19m_0$. For simplicity, we assume AlAs effective masses for both the well (GaAs) and barrier (AlAs), i.e., we consider no effective-mass mismatch.

We now may analyze our results in terms of in-plane (m^*_x and m^*_y) and growth-direction (m^*_z) effective masses. The first important consequence that we notice is that the in-plane effective masses are isotropic for the X_z valley but are anisotropic for the $X_{x,y}$ valleys. Due to this anisotropy, the $2p_x$ and $2p_y$ states of the $X_{x,y}$ valleys are not degenerate. On the other hand, the $2p_x$ and $2p_y$ states of the X_x valley have the same binding energy of the $2p_y$ and $2p_x$ state of the X_y valley, respectively. Therefore, we will discuss only the X_x valley, keeping in mind that this valley is equivalent to the X_y by changing $x \leftrightarrow y$.

In Fig. 2 we show the binding energies for a donor located at the center of the AlAs layer as a function of the layer width for X_z and X_x valleys. For the X_x valley, the combined quantum confinement and anisotropy of the in-plane m^*_x and m^*_y effective masses results into a complete splitting of the $2p$ degeneracy into $2p_x$, $2p_y$, and $2p_z$ states. However, for the X_z valley the in-plane effective masses are isotropic and therefore the $2p_x$ binding energy is degenerate with $2p_y$, a fact that we denote by labeling these binding energies as $2p_{x,y}$. Note that the different effective masses considered have important qualitative and quantitative effects on the binding energies. The most dramatic result is the $2p_z$ state for X_x valley: If calculated with a FR effective mass it is *unbound* for the range of AlAs layer widths considered, whereas it is *bound* when a CR effective mass is used. In general, the $2p_z$ state is unbound for small AlAs layers, which is also observed in type-I quantum wells.[2] Comparing the different valleys, one observes that the $2s$ state has a smaller binding energy than the $2p_x$ state for X_x, while for X_z in general the opposite of true. For the $2p_y$ state, the lighter mass along the y direction at the X_x valley allows the wave function to spread more freely along this direction, becoming virtually independent from the quantum confinement and hence from the AlAs layer width. Therefore, we obtain an almost constant and small binding energy for the $2p_y$ state. For donors located at the edge of the quantum well (Fig. 3) we observe the same strong dependence on the effective mass. The explanation for these very different behaviors of the binding energies follows from a nontrivial interplay between effective masses (CR or FR), effective-mass anisotropy, quantum confinement, and symmetries of the impurity trial functions. For instance, the lighter FR effective masses allow the impurity wave function to spread over a larger region of the AlAs layer; as an immediate result the binding energies are always much smaller than their CR effective mass counterparts. For the X_z valley the in-plane mass is the lighter transversal mass of the bulk X valley [see Table I and Eq. (1)], which allows the wave functions to spread even more along the unconfined x-y plane, thus yielding the smallest binding energies. Such a behavior is observed in type-I structures for quantum wires[20] or dots[21] with applied electric or magnetic fields. In our case this is due to the strong anisotropy of the effective masses and for the type-I quantum wires and dots it is due to the strong asymmetry of the wave functions caused by the external field.

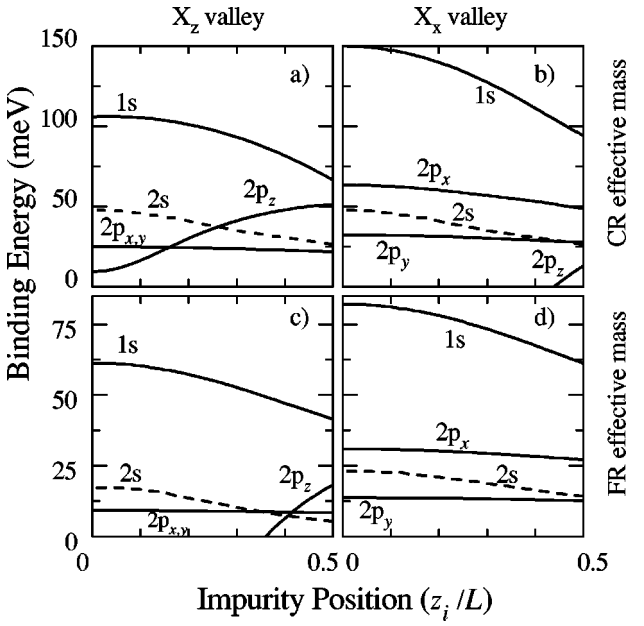

FIG. 4. Binding energies of donors for a 20-Å AlAs layer width as a function of the impurity position z_i in the layer. (a) X_z and (b) X_x valleys calculated with CR effective mass and (c) X_z and (d) X_x valleys calculated with FR effective mass. The $2s$ binding energy is set as a dashed curve for clarity.

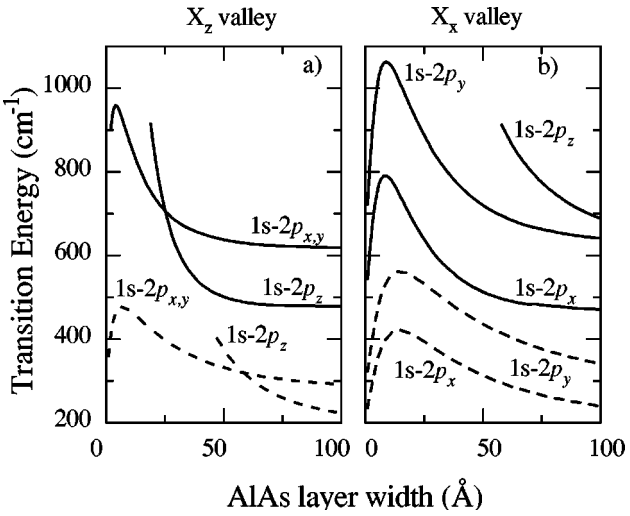

FIG. 5. $1s \rightarrow 2p$ transition energies of donors located at the center ($z_i = 0$) of the AlAs layer as a function of the layer width for (a) X_z and (b) X_x valleys. Solid curves (dashed curves) are for CR (FR) effective masses.

The dependence of the binding energies on the donor impurity position z_i is shown in Fig. 4 for a AlAs layer of 20 Å. The binding energy $2p_z$ state for X_z valleys and CR effective mass [Fig. 4(a)] increases as the donor approaches the interface, which is similar to the behavior of the $2p_z$ in type-I quantum wells.[2] For the other three situations studied the $2p_z$ is mostly unbound, except close to the interface for X_z^{FR} and X_x^{CR}.

In Fig. 5 we show the transition energies for $1s \rightarrow 2p$ transitions for donor located at the center of the AlAs layer. These energies lie in the range 200–1000 cm^{-1}, which is much higher than intradonor transitions in any type-I quantum structure (even wires or dots, provided there is no strong magnetic field).[22–30] Furthermore, the $1s \rightarrow 2p$ transition energies have a strong dependence on the valley (X_z or X_x) and on the effective mass considered. This suggest that a clear distinction of valleys and effective masses could possibly be observed with careful infrared absorption measurements.

At the moment we are not aware of measured excited X valley donor binding energies for GaAs-AlAs type-II structures. However, for the $1s$ state the photoluminescence measurements by Lee *et al.*[12] revealed a binding energy of 104 meV for a large AlAs layer of 131 Å, which is in good agreement with our previously calculated binding energy of 97 meV for X_z^{1s} and 102 meV for X_x^{1s} and indicates that, for these measurements, the heavier CR effective masses may represent more adequately the measured binding energies.

IV. CONCLUSIONS

Our results show that the two sets of effective masses studied in this work provide very different binding energies for ground and excited states of donors linked to X valleys and that these binding energies are quite sensitive to the effective masses that are used in the calculation. Also, the calculated binding energies are remarkably deep when compared to the type-I donors[2] and indicate that even if the GaAs-AlAs structure is of type I there may be X valley donors at lower energies than the confined Γ states or Γ valley donors. For $X_{x,y}$ valleys a complete lifting of the $2p$ degeneracy is obtained that is not observed in unperturbed type-I quantum wells. We believe that the present work may be valuable for further experimental studies on X valley donors and may be helpful in order to clarify the issue of the different effective masses measured for the AlAs X valleys.

ACKNOWLEDGMENTS

G.W. acknowledges financial support from Fapesp (Contract No. 95/9437-2), CNPq (Contract No. 522789/96-0), and Pepci/USF.

[1] E. R. Glaser, T. A. Kennedy, B. Molnar, R. S. Sillmon, M. G. Spencer, M. Mizuta, and T. F. Kuech, Phys. Rev. B **43**, 14 540 (1991).

[2] G. N. Carneiro, G. Weber, and L. E. Oliveira, Semicond. Sci. Technol. **10**, 41 (1995).

[3] A. Latgé, N. Porras-Montenegro, and L. E. Oliveira, Phys. Rev. B **51**, 2259 (1995).

[4] Y.-H. Chang, B. D. McCombe, J.-M. Mercy, A. A. Reeder, J. Ralston, and G. A. Wicks, Phys. Rev. Lett. **61**, 1408 (1988).

[5] S. Huant, W. Knap, G. Martinez, and B. Etienne, Europhys. Lett. **7**, 159 (1988).

[6] P. W. Barmby, J. L. Dunn, and C. A. Bates, J. Phys.: Condens. Matter **6**, 751 (1994).

[7] P. W. Barmby, J. L. Dunn, C. A. Bates, E. P. Pearl, C. T. Foxon,

A. J. van der Sluijs, K. K. Geerinck, T. O. Klaassen, A. van Klarenbosch, and C. J. G. M. Langerak, J. Phys.: Condens. Matter **6**, 7867 (1994).
[8] R. Chen, J.-P. Cheng, D. L. Lin, B. McCombe, and T. F. George, Phys. Rev. B **44**, 8315 (1991).
[9] T. Schmiedel, L. P. Fu, S. T. Lee, W. Y. Yu, A. Petrou, M. Dutta, J. Pamulapati, P. G. Newman, and J. Boviatsis, J. Appl. Phys. **74**, 2100 (1993).
[10] P. Sellitto, J. Sicart, and J. L. Robert, J. Appl. Phys. **75**, 7356 (1994).
[11] P. Sellitto, P. Jeanjean, J. Sicart, J. L. Robert, and R. Planel, J. Appl. Phys. **74**, 7166 (1993).
[12] S. T. Lee, A. Petrou, M. Dutta, J. Pamulapati, P. G. Newman, and L. P. Fu, Phys. Rev. B **51**, 1942 (1995).
[13] A. T. da Cunha Lima, I. C. da Cunha Lima, and A. Ferreira da Silva, Phys. Rev. B **55**, 15 420 (1997).
[14] G. Weber, Appl. Phys. Lett. **67**, 1447 (1995).
[15] M. Goiran, J. L. Martin, J. Leotin, R. Planel, and S. Askenazy, Physica B **177**, 465 (1992).
[16] B. Rheinländer, H. Neumann, P. Fischer, and G. Kühn, Phys. Status Solidi B **49**, K167 (1972).
[17] *Semiconductors: Physics of Group IV Elements and III-V Compounds*, edited by O. Madelung, M. Schulz, and H. Weiss, Landolt-Börnstein, New Series, Group III, Vol. 17, Pt. a (Springer-Verlag, Berlin, 1982).
[18] L. Hsu, S. Zehender, E. Bauser, and E. E. Haller, Phys. Rev. B **55**, 10 515 (1997).
[19] A. M. de Paula and G. Weber, Appl. Phys. Lett. **65**, 1281 (1994).
[20] A. Latgé, N. Porras-Montenegro, and L. E. Oliveira, Phys. Rev. B **45**, 9420 (1992).
[21] C. A. Duque, A. L. Morales, A. Montes, and N. Porras-Montenegro, Phys. Rev. B **55**, 10 721 (1997).
[22] R. L. Greene and K. K. Bajaj, Phys. Rev. B **31**, 913 (1985).
[23] N. Nguyen, J. X. Zang, R. Ranganathan, B. D. McCombe, and M. L. Rustgi, Phys. Rev. B **48**, 14 226 (1993).
[24] Q. X. Zhao, A. Pasquarello, P. O. Holtz, B. Monemar, and M. Willander, Phys. Rev. B **50**, 10 953 (1994).
[25] J. M. Shi, F. M. Peeters, and J. T. Devreese, Phys. Rev. B **50**, 15 182 (1994).
[26] T. Kuhn, G. Mahler, J. L. Dunn, and C. A. Bates, J. Phys.: Condens. Matter **6**, 757 (1994).
[27] M. El-Said, Physica B **202**, (1994).
[28] P. D. Emmel, J. R. Leite, and I. C. da Cunha Lima, Phys. Rev. B **43**, 9265 (1991).
[29] S. V. Branis, G. Li, and K. K. Bajaj, Phys. Rev. B **47**, 1316 (1993).
[30] E. R. Mueller, W. D. Goodhue, D. M. Larsen, J. W. Bales, and J. Waldman, Phys. Rev. B **44**, 1754 (1991).